JET-P(96)50

Interpretation of Measurements of ICRF-heated Minority Proton Distributions in JET

K G McClements[1], R O Dendy[1], A Gondhalekar.

JET Joint Undertaking, Abingdon, Oxfordshire, OX14 3EA, UK.
[1] UKAEA Fusion, Culham, Abingdon, Oxfordshire, OX14 3DB, UK.
(UKAEA/Euratom Fusion Association)

Preprint of a paper submitted for publication in
Nuclear Fusion

November 1996

ABSTRACT

In the JET tokamak, the perpendicular velocity distribution function of minority ICRF-heated protons in the MeV energy range is inferred from neutral particle analyzer (NPA) measurements of the emitted hydrogen flux, integrated along a vertical line-of-sight through the plasma centre. In particular, the best-fit perpendicular tail temperature $\tilde{T}_\perp$ of the inferred distribution can be determined with good accuracy. In this paper a relation is established between the measured quantity $\tilde{T}_\perp$ and the perpendicular tail temperature $T_\perp(0)$ of the heated protons at the position of maximum ICRF power deposition. If measurements are made at energies E which lie well above $T_\perp(0)$, the value of $\tilde{T}_\perp$ inferred from the NPA measurements is only slightly lower than $T_\perp(0)$. In the opposite limit $E << T_\perp(0)$, it is shown that $\tilde{T}_\perp << T_\perp(0)$. When this model is applied to NPA measurements from a JET pulse with varying levels of applied ICRF power P_{RF}, it is found that the scaling of $T_\perp(0)$ with P_{RF} in the 2-10 MW range is almost exactly linear, as expected from the widely-used Stix model. Moreover, calculated values of the ICRF-heated proton energy content, based on deduced values of $T_\perp(0)$, are in agreement with independent diamagnetic measurements of the energy. These results validate the model of impurity-induced neutralization of MeV protons which has been developed to interpret NPA flux measurements in JET. The measurements thus give access to a fundamental property of the high energy minority proton energy distribution, which plays a crucial role in theories of sawtooth stabilization. The successful measurement of ICRF-heated proton distributions in the high energy range gives confidence that the NPA instrumentation, and the interpretation techniques described here, could provide valuable data on the behaviour of fusion products in forthcoming deuterium-tritium experiments in JET.

1. INTRODUCTION

Measurements made using a neutral particle analyzer (NPA) have yielded the perpendicular velocity distribution function of protons in the MeV energy range in the Joint European Torus (JET) [1-2]. The protons, which constitute a minority ion species in the predominantly deuterium plasma, are heated by waves in the ion cyclotron range of frequencies (ICRF), and their velocity distribution is strongly anisotropic at energies $E >> E_{crit}$, where E_{crit} is the critical energy at which the electron proton and deuteron-proton collision frequencies are equal [3]. The NPA measurement technique involves detection of high energy hydrogen atoms, formed by neutralization of protons in charge exchange reactions. In the energy range of the NPA, 0.3 MeV $\leq$ E $\leq$ 4 MeV, Korotkov and Gondhalekar [1-2] have recently demonstrated that hydrogen-like ([H]) ions of carbon and beryllium, the main intrinsic plasma impurities in JET, are the dominant contributors to proton neutralization. Using a system of steady-state balance

equations for bare and [H] impurity ions, Korotkov et al. showed that high densities of [H] ions of carbon and beryllium occur in the core region of JET plasmas. The required cross-sections for neutralization of protons by [H] impurity ions have not been measured, and were therefore taken from theoretical calculations. In Refs [1] and [2] the proposed model of impurity induced neutralization (IIN) was tested by using it to describe the evolution of the NPA-measured hydrogen flux in different conditions of plasma heating and fueling. In this paper, we seek further validation of the IIN modelling by using NPA measurements to estimate the energy content of ICRF-heated protons, and by comparing such estimates with independent diamagnetic measurements of the fast proton energy content.

The energy range of the measurements reported in this paper is 0.3 MeV - 1.1 MeV. The measured quantity $\tilde{\Gamma}$ the flux of hydrogen atoms arriving at the NPA per unit area per unit energy, is proportional to the line integral of the local proton energy distribution F_h, weighted with respect to the local proton neutralization probability per unit time P_v,. Thus, we have

$$\tilde{\Gamma}(E) = \int_{-b}^{b} P_v(E, Z) F_h(E, Z) dZ, \tag{1}$$

where E is the energy of a proton moving towards the NPA, Z is vertical coordinate, and b is the height of the plasma along the NPA line-of-sight. We can define a line integrated distribution function $\tilde{F}_h(E)$ by writing

$$\tilde{F}_h(E) \equiv \frac{\tilde{\Gamma}(E)}{P_v(E, 0)} = \frac{1}{P_v(E, 0)} \int_{-b}^{b} P_v(E, Z) F_h(E, Z) dZ. \tag{2}$$

In Refs [1] and [2], $P_v(E, 0)$ was calculated for the plasma core using computed cross-sections which are known to an accuracy of between 10% and 30%, depending on proton energy and the nuclear charge of the impurity species with which the protons interact. In general, P_v is an extremely complicated function of Z. However, the radial profiles of the parameters upon which P_v depends all have characteristic scale lengths of the order of b, whereas the scale length of F_h is smaller than the width of the ICRF power deposition profile, which in turn is much smaller than b (see below). Thus, it is reasonable to set $P_v(E, Z)$ equal to $P_v(E, 0)$ in Eq. (2), so that $\tilde{F}_h(E)$ is simply the line integral of the local distribution $F_h(E, Z)$. Korotkov et al. [1-2] assumed a Maxwellian energy distribution, i.e. a relation of the form $\tilde{F}_h \propto E^{1/2} \exp\left(-E/\tilde{T}_\perp\right)$, and used a least-squares procedure to deduce best-fit temperatures $\tilde{T}_\perp$ lying typically in the range 100-300 keV for ICRF powers in the range 2-10 MW.

Accurate measurements of minority ICRF-heated ion distributions are important for several reasons. Firstly, such measurements provide a useful method of testing theories of ICRF power deposition. Secondly, there is a well-established link between ICRF-heated ions

and magnetohydrodynamic (MHD) activity; for example, ICRF heating has stabilized sawtooth oscillations in JET [4]. Finally, if a reliable technique could be developed for deducing ICRF-heated ion distributions, such a technique could then be applied with confidence to measuring the energy distributions of fusion products in forthcoming deuterium-tritium experiments in JET.

In this paper we provide a physical interpretation of the measured quantity $\tilde{T}_\perp$, and confront that interpretation with independent experimental data on ICRF-heated protons. In Section 2 we derive an expression for the local energy distribution of protons whose velocity vectors are such that they would, if neutralized, be detected by the NPA. In Section 3 we use this expression to infer a relation between the measured temperature $\tilde{T}_\perp$ and the local proton tail temperature at the position of maximum ICRF power deposition. This result enables us to calculate the proton energy content. As noted above, by comparing such estimates with independent diamagnetic measurements of the total proton energy, it is possible to test the IIN model proposed in Refs [1] and [2]. Our conclusions are briefly summarized in Section 4.

2. LOCAL PROTON ENERGY DISTRIBUTION

In the energy range of the measurements described in Refs [1] and [2], we adopt a bi-Maxwellian model for the local anisotropic velocity distribution of ICRF-beated minority protons, i.e.

$$f_h(\mathbf{v},Z)=\frac{n_h(Z)m_p^{3/2}}{(2\pi)^{3/2}T_{\|}(Z)^{1/2}T_\perp(Z)}\exp\left(-\frac{m_p\left(v_z^2+v_y^2\right)}{2T_\perp(Z)}-\frac{m_pv_x^2}{2T_{\|}(Z)}\right), \tag{3}$$

where $n_h(Z)$ is the local proton density, m_p is the proton mass, $T_{\|}(Z)$ and $T_\perp(Z)$ are local temperatures parallel and perpendicular to the magnetic field, which lies in the x-direction. We assume that the poloidal component of the field can be neglected, so that one of the velocity space directions (z) can be identified with the vertical coordinate space direction Z. If the entire proton distribution is rotating toroidally with flow velocity v_f, the velocity component v_x in Eq. (3) should be replaced with v_x - v_f. Only atoms with $v_z/\left(v_x^2+v_y^2\right)^{1/2}\gtrsim 200$ can enter the NPA [1-2], and the velocity vector of a proton is not significantly changed by the capture of an electron. Thus, the velocity distribution of protons which, if neutralized, can be detected by the NPA is given by

$$\tilde{f}_h(v_z,Z)=\iint dv_xdv_yf_h(\mathbf{v})=\int_0^{2\pi}d\phi\int_0^{v_z/200}v_\phi dv_\phi f_h(\mathbf{v},Z), \tag{4}$$

where $v_\phi = \left(v_x^2 + v_y^2\right)^{1/2}$ and ϕ = $\tan^{-1}$ (v_y/v_x). Given that $T_\perp$ and $T_{||}$ exceed the electron temperature T_e ~ 5 - 10 keV [4], and that $m_p v_z^2/2 \lesssim 4\text{MeV}$, it is straightforward to verify that $v_z/200$ is much smaller than $\left(2T_\perp/m_p\right)^{1/2}$ and $\left(2T_{||}/m_p\right)^{1/2}$, and so, for $0 \le v_\phi \le v_z/200$, the function $f_h(\mathbf{v})$ depends only on v_z. This remains true if $v_f \neq 0$, provided that $m_p v_f^2 << 2T_{||}$, which is invariably the case in JET [5]. Equation (4) thus yields

$$\tilde{f}_h(v_z, Z) = \frac{v_z^2 n_h(Z) m_p^{3/2}}{200^2 2^{3/2} \pi^{1/2} T_{||}(Z)^{1/2} T_\perp(Z)} \exp\left(-\frac{m_p v_z^2}{2T_\perp(Z)}\right) \tag{5}$$

Using the fact that the measured hydrogen atom energy E is approximately equal to $m_p v_z^2/2$, and defining an energy distribution function $F_h(E,Z)$ by writing $F_h(E,Z)dE = \tilde{f}_h(v_z, Z)dv_z$, we infer that the local energy distribution of protons which can be detected by the NPA is of the form

$$F_h(E, Z) = \frac{C_0 E^{1/2}}{T_\perp(Z)} \exp\left(-\frac{E}{T_\perp(Z)}\right) \tag{6}$$

where $C_0 \propto n_h(Z)/T_{||}(Z)^{1/2}$. Stix [3] predicted that ICRF-heated ions would have a tail distribution of this form, the energy density $n_h T_\perp$ being approximately equal to $\rho_{RF}\tau_s$ where ρ_{RF} is the ICRF wave power density coupled to minority ions and τ_s is the collisional slowing-down time. Physically, this result arises from a balance between minority ion cyclotron damping of the ICRF waves and collisional heating of electrons by minority ions. The expression obtained by Stix for $T_\perp$ has been widely used in the interpretation of ICRF heating experiments [6-7], but has only recently been recognized as a key parameter in theories of ICRF-induced sawtooth stabilization [8-9]. The purpose of this paper is to establish a method of deducing $T_\perp$ at the position of maximum ICRF power deposition from line-integrated measurements of ICRF-heated proton energy distributions. We note that the quantity F_h defined by Eq. (6) is so far a theoretical construct, whereas the quantity $\tilde{F}_h$ defined by Eq. (2) can be inferred from measurements.

Ray-tracing and full wave calculations for JET indicate that ρ_{RF} has a Gaussian radial profile, which is generally sharply peaked in the plasma centre with an e-folding width of the order of 20-30 cm [10]. Detailed calculations indicate that the variation of ρ_{RF} with minor radial distance r can be well-represented by a Gaussian (see e.g. Fig.5 in Ref. [10]), in which case $n_h T_\perp \sim \rho_{RF}\tau_s$ yields an expression for $T_\perp(z)$of the form [7]

$$T_\perp(Z) = \frac{\rho_0 \tau_s(Z)}{n_h(Z)} \exp\left(-\frac{Z^2}{D^2}\right) \tag{7}$$

Here D is a vertical length scale associated with the radial profile of ρ_{RF}, ρ_0 is a constant with the dimensions of power density, and the slowing-down time $\tau_s \propto T_e^{3/2}/n_e$ where T_e, n_e are electron temperature and density. In ICRF-heated plasmas, T_e is generally more strongly-peaked than n_e (see, e.g., Fig.3 in Ref. [6]), and so the scale length associated with τ_s may be somewhat smaller than b. However, n_h is likely to have a radial profile which is similar to that of n_e, and so we would expect $\tau_s/n_h \propto T_e^{3/2}/n_h$ to have a scale length of the order of b. Thus, the radial profile of $T_\perp$ is determined essentially by the value of $D << b$, and Eq. (7) can be well-approximated by the expression

$$T_\perp(Z) = T_\perp(0) \exp\left(-\frac{Z^2}{D^2}\right). \tag{8}$$

Our aim is now to combine Eq. (6) with Eqs (7) and (8), to obtain an expression for the model line-integrated proton distribution function which can be compared to the measured one defined in Eq. (2). The normalization parameter C_0 in Eq. (6) is proportional to $n_h/T_{||}^{1/2}$, and is thus dependent on Z. In the model developed by Stix [4], $T_{||} \propto T_e$ which implies that C_0, like τ_s/n_h has a much longer scale length than $T_\perp$. Moreover, at suprathermal energies $E > T_\perp(Z)$, the presence of an exponential factor in both Eq. (6) and Eq. (8) means that the spatial variation of F_h is more rapid than that of $T_\perp$: a small change in $T_\perp$ corresponds to a very large change in F_h. It is justifiable, therefore, to treat C_0 in Eq. (6) as a constant henceforward.

3. LINE-INTEGRATED PROTON ENERGY DISTRIBUTION

The following question naturally arises: what is the relation between the measured temperature $\tilde{T}_\perp$ and $T_\perp(Z)$? In particular, does $\tilde{T}_\perp$ give a measure of the actual proton tail temperature in the centre of the ICRF power deposition region, or at the edge of that region? With F_h given by Eq.(6), and $T_\perp(Z)$ given by Eq. (8), the integral in Eq. (2) may be exactly evaluated numerically, and is also tractable analytically to a considerable extent. We consider the equivalent dimensionless integral

$$\tilde{F}(\varepsilon) = \varepsilon^{1/2} \int_0^\infty \exp\left(\xi^2 - \varepsilon e^{\xi^2}\right) d\xi. \tag{9}$$

Here, $\varepsilon = E/T_\perp(0)$ and $\xi = Z/D$. The fact that $D << b$ makes it possible to replace the finite interval of integration in Eqs. (1) and (2) with a semi-infinite interval in Eq. (9). A log-linear plot of $\tilde{F}(\varepsilon)/\varepsilon^{1/2} (0 < \varepsilon \leq 10)$ is shown as a solid line in Fig.1: for suprathermal values of $\varepsilon >> 1$, we see that $\tilde{F}/\varepsilon^{1/2}$ falls off roughly exponentially with ε. This can be demonstrated analytically by setting $e^{\xi^2} \simeq 1 + \xi^2 + \xi^4/2$ in Eq. (9), which yields the tractable approximation

$$\frac{\tilde{F}(\varepsilon)}{\varepsilon^{1/2}} \simeq 2^{-3/2}\left(1-\frac{1}{\varepsilon}\right)^{1/2}\exp\left[\frac{\varepsilon}{4}\left(1-\frac{1}{\varepsilon}\right)^2-\varepsilon\right]K_{1/4}\left[\frac{\varepsilon}{4}\left(1-\frac{1}{\varepsilon}\right)^2\right] \simeq \frac{1}{2}\left(\frac{\pi}{\varepsilon}\right)^{1/2}e^{-\varepsilon}\left\{1+\frac{1}{8\varepsilon}\right\}, \quad (10)$$

where $K_{1/4}$ is a modified Bessel function of the second kind. To obtain Eq. (10) we have used Eqs. (3.323) in Ref. [11] and (9.7.2) in Ref. [12], expanding $\tilde{F}(\varepsilon)/\varepsilon^{1/2}$ to first order in $\frac{1}{\varepsilon}$. The final expression in Eq. (10) is represented by a dashed line in Fig. 1: it is distinguishable from the exact numerical result (the solid line) only at $\varepsilon \lesssim 1$. Thus, Eq. (10) provides an extremely good approximation to $\tilde{F}(\varepsilon)$ defined by Eq. (9), even in the low energy limit.

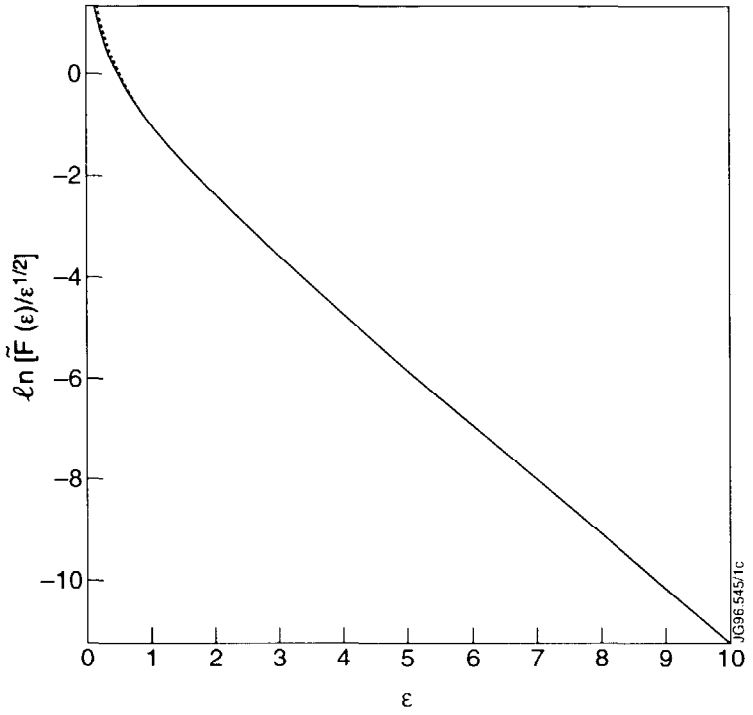

Fig.1: Solid curve: the function $\tilde{F}(\varepsilon)/\varepsilon^{1/2}$ defined by Eq. (9), for $0 < \varepsilon < 10$. Dashed curve: the approximate form of $\tilde{F}(\varepsilon)/\varepsilon^{1/2}$ given by the second equality in Eq. (10). The dimensionless parameter ε is equal to $E/T_\perp(0)$ and $\tilde{F}$ is a measure of the line-integrated (measured) minority ion distribution. The two curves begin to diverges only at $\varepsilon \lesssim 1$, indicating that Eq. (10) is an extremely accurate approximation to $\tilde{F}(\varepsilon)/\varepsilon^{1/2}$ in the energy range of the measurements.

Korotkov et al. [1-2] obtained a set of best-fit temperatures $\tilde{T}_\perp$ corresponding to various levels of applied ICRF power in a single pulse. For each power level in the range 2-10 MW, they fitted a single Maxwellian to the line-integrated proton distribution over the entire energy range of the measurements: each best-fit temperature is thus a global parameter of the corresponding proton distribution. The distribution given by Eq. (10) is not a single temperature Maxwellian, since it does not have a simple $\varepsilon^{1/2}e^{-\varepsilon}$ dependence. Such a dependence would imply $\tilde{T}_\perp = T_\perp(0)$, since , $\varepsilon = E/T_\perp(0)$ and $\tilde{T}_\perp$ is defined by

$\tilde{F}_h \propto E^{1/2} \exp\left(-E/\tilde{T}_\perp\right)$. In general, it is possible to define an energy-dependent temperature $\bar{T}_\perp$ in the neighbourhood of a given value of E by writing

$$\bar{T}_\perp(\varepsilon) \equiv -\frac{T_\perp(0)}{d\ln\left(\tilde{F}/\varepsilon^{1/2}\right)/d\varepsilon}. \tag{11}$$

The quantity $\bar{T}_\perp(\varepsilon)$ can be related to the observed temperature $\tilde{T}_\perp$ as follows. The true line-integrated distribution $\tilde{F}_h(E)$ defined by Eq. (2), which we assume to have the same shape as the function $\tilde{F}(\varepsilon)$ defined by Eq. (9), is plotted schematically as a solid curve in Fig.2 for $E_{\min} \le E \le E_{\max}$: $E_{\min}$ and $E_{\max}$ represent the limits of the measured energy range. The dashed line represents the best-fit single Maxwellian over that range, with slope $-\tilde{T}_\perp^{-1}$ (the difference between the two curves has been exaggerated for clarity). Clearly, the best-fit single Maxwellian will intersect with $\tilde{F}_h(E)$ at energies E_1 and E_2 which lie within the observed range, and the mean-value theorem implies that the gradients of the two curves must coincide at an energy E_* such that $E_1 < E_* < E_2$. At that energy, it follows from Eq. (11) that $\bar{T}_\perp\left(E_*/T_\perp(0)\right) = \tilde{T}_\perp$. Obviously E_* must lie within the 300-1100 keV range of the measurements: for simplicity, we set E_* equal to the median energy of 650 keV.

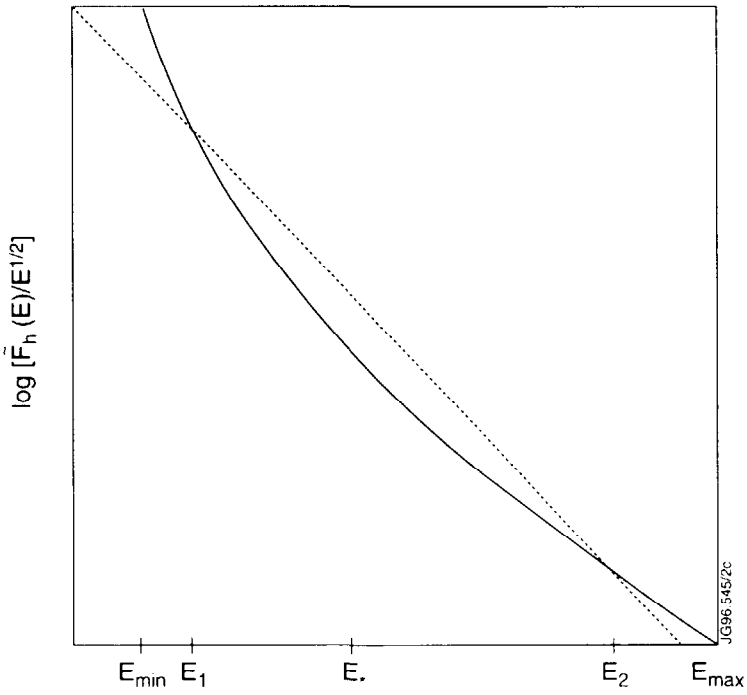

Fig.2: Solid curve: schematic plot of $\log\left[\tilde{F}_h(E)/E^{1/2}\right]$. *Dashed curve: single-Maxwellian fit to* $\tilde{F}(E)/E^{1/2}$ *over the energy range* $E_{\min}$ *to* $E_{\max}$. *The two curves intersect at* E_1 *and* E_2, *and, according to the mean-value theorem, have equal gradients at* E_* *such that* $E_1 < E_* < E_2$. *At that energy, the effective temperature* $\bar{T}_\perp$ *defined by the slope of* $\log\left(\tilde{F}_h(E)/E^{1/2}\right)$ *is equal to the measured temperature* $\tilde{T}_\perp$.

The function defined by Eq. (11) is plotted in Fig.3. When $\varepsilon >> 1$, i.e. $E >> T_\perp(0)$, the temperature ratio tends to one. In such cases, the effective temperature $\bar{T}_\perp$ of the line-integrated minority ion distribution is only slightly lower than the local tail temperature $T_\perp(Z)$ in the plasma centre ($Z = 0$). When $\varepsilon \lesssim 1$, on the other hand, $\bar{T}_\perp$ is significantly lower than $T_\perp(0)$. We can derive an explicit expression for $T_\perp(0)$ in terms of E_* and $\tilde{T}_\perp$ as follows. Using the second equality in Eq. (10) to evaluate the derivative in Eq. (11), and recalling that $\varepsilon = E/T_\perp(0)$, we obtain a quadratic equation for $T_\perp(0)$. With E and $\bar{T}_\perp$ respectively set equal to E_* and $\tilde{T}_\perp$, the appropriate solution is

$$T_\perp(0) = 4E_*^2\left[\frac{1}{\tilde{T}_\perp} - \frac{1}{2E_*} - \left(\frac{1}{\tilde{T}_\perp^2} - \frac{1}{E_*\tilde{T}_\perp} - \frac{1}{4E_*^2}\right)^{1/2}\right] \tag{12}$$

To leading order in $\tilde{T}_\perp/E_*$ this reduces to

$$T_\perp(0) \simeq \tilde{T}_\perp\left(1 + \frac{\tilde{T}_\perp}{2E_*}\right) \tag{13}$$

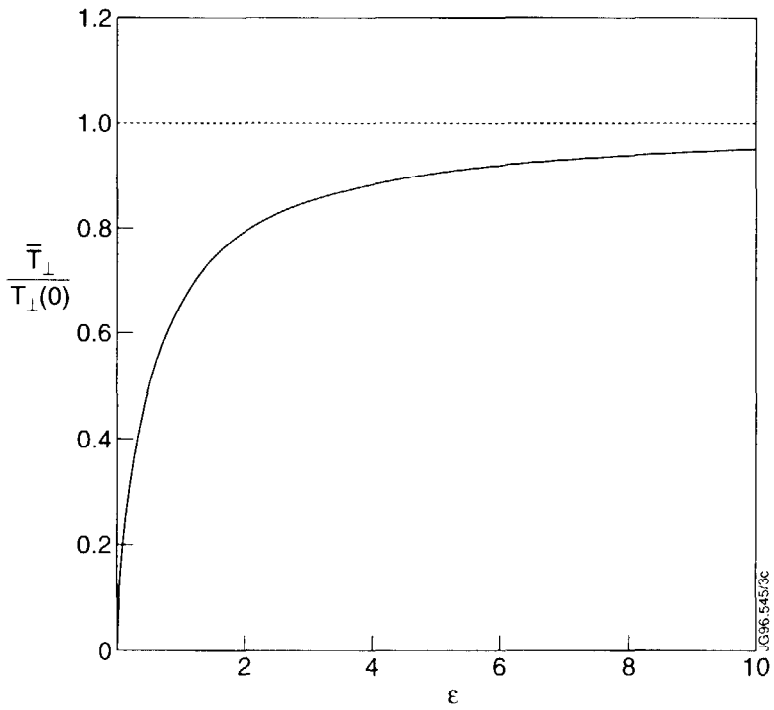

Fig.3: The temperature ratio $\bar{T}_\perp/T_\perp(0)$ as a function of $\varepsilon \equiv E/T_\perp(0)$. Here, $\bar{T}_\perp(\varepsilon) \equiv -T_\perp(0)\Big/\left(d\ln\left(\tilde{F}/\varepsilon^{1/2}\right)/d\varepsilon\right)$ is the effective temperature of the line-integrated proton distribution: it is energy-dependent, and is equal to the measured temperature $\tilde{T}_\perp$ at an energy E_* lying within the range of the measurements. When $E_* >> T_\perp(0)$, the measured temperature is approximately equal to $T_\perp(0)$.

Equations (12) and (13) enable us to estimate the peak tail temperature of the protons from the NPA measurements. In the case of the distribution function data shown in Fig.15 of

Ref. [2], the best-fit values of $\tilde{T}_\perp$ range from 80 keV for 2 MW ICRF heating power, to 265 keV for 10 MW ICRF heating power. Setting $E_* = 650$ keV, we find that Eq. (12) gives $T_\perp(0) \simeq 85.4$ kev when $\tilde{T}_\perp = 80$ keV, and $T_\perp(0) \simeq 344.5$ keV when $\tilde{T}_\perp = 265$ keV. The Stix model [3] implies that $T_\perp(0)$ should increase linearly with the ICRF power density which is coupled to the minority ions, ρ_{RF}. This does not necessarily imply a linear relation between $T_\perp(0)$ and the total ICRF power P_{RF}, since the radial profile of the latter (and hence ρ_{RF}) is affected by the minority ion distribution, and in any case the fraction of P_{RF} which is coupled to minority ions is itself a weak function of P_{RF} [10]. Nevertheless, we would expect $T_\perp(0)$ to scale with $(P_{RF})^\alpha$ where $\alpha \simeq 1$. In fact, usingEq. (12) to obtain a set of values of $T_\perp(0)$ from the observed values of $\tilde{T}_\perp$ in Fig.15 of Ref. [2], we find that $T_\perp(0) \propto (P_{RF})^{0.89\pm0.06}$: this compares with $\tilde{T}_\perp \propto (P_{RF})^{0.77\pm0.06}$. Thus, the measured scaling of peak minority ion tail temperature with ICRF power is almost exactly linear. In this respect the Stix model is in good agreement with the corrected proton tail temperature.

Having inferred the peak proton tail temperature $T_\perp(0)$ corresponding to a particular ICRF power level, we can now calculate the total proton energy W_p for comparison with values obtained from diamagnetic measurements [6]. It is straightforward to show that the local energy density of a bi-Maxwellian proton distribution with parallel and perpendicular temperatures $T_{||}$, $T_\perp$ is

$$u = n_h T_\perp \left(1 + \frac{T_{||}}{2T_\perp}\right), \tag{14}$$

where, as before, n_h is the proton number density. The NPA measurements described in Refs [1] and [2] do not provide any information on $T_{||}$, but it is reasonable to assume that $2T_\perp >> T_{||}$ [4], so that $u \simeq n_h T_\perp$. We assume, for simplicity, that u is only weakly dependent on poloidal angle: this is justified when $T_{||}/T_\perp$ is greater than the local inverse aspect ratio [9]. The total proton energy is then given by

$$W_p = \int u d^3r \simeq 4\pi^2 R_0 \int_0^a u(r) r dr, \tag{15}$$

where R_0, a are the major and minor radii ($a \simeq b$), and r is minor radial distance. In view of the disparity between ICRF power deposition length scale D and plasma height b noted earlier, we can set $T_\perp = T_\perp(0) \exp\left(-r^2/D^2\right)$ [9] and approximate n_h as a constant, with the upper integration limit in Eq. (15) tending to infinity. We then obtain

$$W_p \simeq 2\pi^2 R_0 D^2 n_h T_\perp(0) \tag{16}$$

Figure 4 shows a comparison between: values of W_p calculated for a series of ICRF-heated JET pulses using Eq. (16), with $T_\perp(0)$ inferred from NPA measurements in the manner described in this paper; and the corresponding measured values of the fast ion energy content W_{fast}, deduced from diamagnetic measurements. The dashed line corresponds to $W_p = W_{fast}$. To evaluate W_p, we have used $R_0 = 3.1$ m and $D = 0.3$ m. The proton density n_h was measured independently, as described in Ref. [13]. The peak proton tail temperature $T_\perp(0)$ was obtained from Eq. (12), using measured values of $\tilde{T}_\perp$ and with $E_* = 650$ keV. The largest source of error in W_p is the proton density n_h, which varies from pulse to pulse [13]. The overall experimental errors in W_{fast} and W_P are shown explicitly for three of the points in Fig.4. In general, D is a function of P_{RF}: our assumption that D is equal to 0.3 m for every pulse thus constitutes an additional source of error. Nevertheless, within the fairly broad limits of experimental uncertainty, it is clear from Fig.4 that our computed values of W_p are consistent with independent measurements of the ICRF-heated ion stored energy.

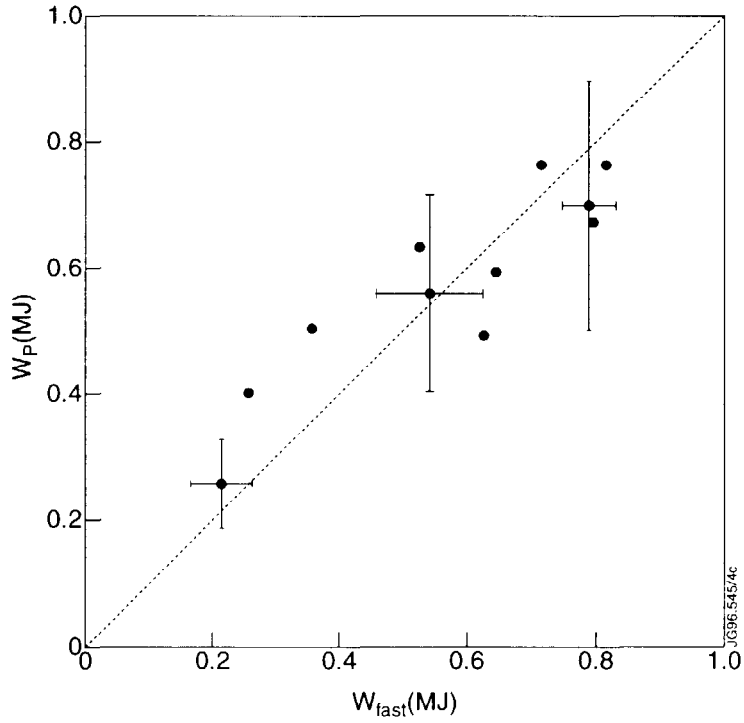

Fig.4: Total proton energy W_p given by Eq. (16), plotted against the proton energy deduced from diamagnetic measurements W_{fast}, for a set of JET pulses with various levels of ICRF power. To compute W_p, we have set $R_0 = 3.1$ m and $D = 0.3$ m. The proton concentration n_h/n_e varies from pulse to pulse. The peak proton tail temperature $T_\perp(0)$ has been obtained from Eq. (12), using measured values of $\tilde{T}_\perp$ and with E_*=650 keV. The dashed line corresponds to $W_p = W_{fast}$. All the data points are subject to error: for clarity, the error bars on only a few of the points are shown. The errors in W_p arise from uncertainties in n_h, $\tilde{T}_\perp$ and D.

This result shows that the inferred $T_\perp(0)$ is the true tail temperature of the ICRF-driven proton energy distribution in the plasma. Moreover, as shown earlier, the scaling of $T_\perp(0)$ with

ICRF power density is in accord with the theory of Stix. Nevertheless, the magnitude of $T_\perp(0)$ and W_p are smaller than those given by the theory as adapted to JET conditions and manifested in the PION code [10]. Reasons for this discrepancy will be discussed in a forthcoming publication [14].

4. CONCLUSIONS

We have proposed a simple model which provides a precise physical interpretation of new ICRF-heated proton tail temperature measurements in JET: the simplicity of the model is in part a consequence of the fact that the length scale associated with spatial variation of the proton distribution is much shorter than that of every other plasma parameter which affects the measurements. We have assumed that the perpendicular velocity distribution of ICRF-heated protons is locally Maxwellian, with a temperature which has a Gaussian radial profile. On that basis, we have shown that the peak proton tail temperature $T_\perp(0)$ has a dependence on ICRF power which is stronger - and more nearly linear - than that of the measured temperature $\tilde{T}_\perp$, and, in this respect, is broadly consistent with the scaling suggested by the model of minority ICRF heating developed by Stix [3]. Moreover, our inferred values of $T_\perp(0)$ are consistent with estimates of the total ICRF-heated proton energy content deduced from diamagnetic measurements, and therefore $T_\perp(0)$ is the true tail temperature of the high energy proton distribution function in the plasma center. However, the magnitude of $T_\perp(0)$ and W_p are smaller than those given by model calculations adapted to JET conditions. Lastly, these results validate the model of impurity-induced neutralization of MeV protons developed by Korotkov et al. [1-2] to interpret NPA flux measurements, and are thus encouraging for the development of the NPA for alpha-particle measurements in forthcoming deuterium-tritium experiments in JET.

ACKNOWLEDGMENTS

We would like to thank L-G. Eriksson and P. R. Thomas for helpful critisism, and to M. J. Mantsinen for PION calculations. This work was funded jointly by the UK Department of Trade and Industry and Euratom.

REFERENCES

[1] KOROTKOV, A.A., GONDHALEKAR, A., in Controlled Fusion and Plasma Physics (Proc 21st Eur. Conf. Montpellier, 1994), Vol. 18B, Part 1, European Physical Society, Geneva (1994) 266.

[2] KOROTKOV, A.A., et al., Impurity Induced Neutralization of MeV Energy Protons in JET Plasmas, JET Report JET-P(95)47; Nucl. Fusion, in press.

[3] STIX, T.H., Nucl. Fusion **15** (1975) 737.

[4] CAMPBELL, D.J., et al., Phys. Rev. Lett **60** (1988) 2148.
[5] SNIPES, J.A., et al., Nucl. Fusion **28** (1988) 1085.
[6] BOYD, D.A., et al., Nucl. Fusion **29** (1989) 593.
[7] COTTRELL, G.A., START, D.F.H., Nucl. Fusion **31** (1991) 61.
[8] DENDY, R.O., et al., Phys. Plasmas **2** (1995) 1623.
[9] McCLEMENTS, K.G., et al.,, UKAEA FUS 326; Phys. Plasmas **3** (1996) 2994.
[10] ERIKSSON, L.-G., HELLSTEN, T., Phys. Scr. **52** (1995) 70.
[11] GRADSHTEYN, I.S., RYZHIK, I.M., Table of Integrals, Series, and Products, Academic Press, New York (1980).
[12] ABRAMOWITZ, M., STEGUN, I.A., Handbook of Mathematical Functions, Dover, New York (1965).
[13] GÜNTHER, K., et al., Behaviour of Hydrogen in JET Deuterium Plasmas, J. Nucl. Materials in press (Proc. 12th Int. Conf. on Plasma Surface Interactions in Controlled Fusion Devices, St Raphael, 1996).
[14] GONDHALEKAR, A., in preparation.